

## General Disclaimer

### One or more of the Following Statements may affect this Document

- This document has been reproduced from the best copy furnished by the organizational source. It is being released in the interest of making available as much information as possible.
- This document may contain data, which exceeds the sheet parameters. It was furnished in this condition by the organizational source and is the best copy available.
- This document may contain tone-on-tone or color graphs, charts and/or pictures, which have been reproduced in black and white.
- This document is paginated as submitted by the original source.
- Portions of this document are not fully legible due to the historical nature of some of the material. However, it is the best reproduction available from the original submission.

Semi-Annual Report

NASA Grant NSG-5155

Remote Sensing Applications to Hydrologic Modeling

(NASA-CR-154842) REMOTE SENSING N77-30571  
APPLICATIONS TO HYDROLOGIC MODELING  
Semiannual Report (California Univ.) 27 p  
HC A03/MF A01 CSCL 08H Unclas  
G3/43 42141

Principal Investigators

Jeff Dozier  
John E. Estes  
David S. Simonett

Contributing Authors

Robert Davis  
James Frew  
Danny Marks  
Karl Schiffman  
Mary Souza  
Ellen Witebsky

Department of Geography  
University of California  
Santa Barbara  
September 1977

c

Contents

I.	Summary of Accomplishments	- 1
II.	Discussion of Tasks Underway	- 4
	A. An Energy Balance Snowmelt Model for Rugged Terrain	- 4
	1. Development and Testing of Wavelength-Dependent Topographic Solar Radiation Algorithms	- 4
	2. Shortwave Albedo of an Extensive Snow Cover Derived from Landsat Data	- 6
	3. Development and Testing of Longwave Radiation Algorithms	- 9
	4. Possible Approaches to Wind Interpolation	- 11
	5. Flow Diagrams of Snowmelt Model Structure	- 13
	B. Coupling Snowmelt Model to Flow Model	- 15
	1. Review of Literature on Frost Penetration and its Hydrologic Effects	- 15
	2. Development of Geocoded Hydrologic Information System	- 15
	3. Development of Flow Model for Snowmelt	- 16
	C. Literature Review on Remote Sensing Applications to Hydrologic Modeling	- 17
	1. Development of Bibliography and Computerized Retrieval System	- 17
	2. Future Remote Sensing Applications to Hydrologic Modeling	- 17
III.	Software Development	- 19
IV.	Accomplishments Forseen by End of First Year of Grant and Recommendations for Further Work	- 24
V.	References	- 25

## I. SUMMARY OF ACCOMPLISHMENTS

1. Assembly of data and hydrologic and physiographic descriptions of the Soviet and U.S. test sites.

The following documents have been prepared for presentation to the NASA technical monitor:

a. A geographic description of the Fergana Valley test site was sent to the NASA Technical Monitor in April 1977. This description will be updated, including information from the Soviet description, for the final report.

b. A geographical description of the southern Sierra Nevada/San Joaquin Valley test site was sent to the NASA Technical Monitor in June 1977.

c. Numerous field measurements of solar radiation and snow reflectance taken during the 1976-77 snow season have been tabulated and stored as a computer text file. Printed copies of this data are available upon request and will be included with the final report.

d. Field measurements of air temperature, vapor pressure, surface temperature, and incoming atmospheric radiation, taken during the 1976-77 snow season, have also been tabulated and stored as a computer text file. Printed copies of this data are available upon request and will be included in the final report.

2. Development of energy-balance snowmelt model for large mountainous area.

a. Development of wavelength-dependent topographic solar radiation algorithms.

i. Method of calculating absorption and scattering coefficients and portion of radiation scattered forward has been completed.

ii. These coefficients and terrain information are used to produce maps of solar radiation. At present the algorithm does not include non-Lambertian reflectance from adjacent slopes, but this modification is under development.

iii. Numerous (over 400) field measurements of incoming and reflected radiation have been made, for calibration and verification of algorithms.

b. Determination of snow reflectance from Landsat.

i. We have adapted DIRS software to our computer system and have identified suitable ground control points within study area.

ii. A program to map space radiance values corresponding to incoming solar radiation has been developed.

iii. We have necessary field data to apply standard atmospheric corrections.

c. Temperature and humidity estimates.

i. An algorithm for interpolating temperature and vapor pressure over a topographic surface from a few discontinuous measurements has been developed.

ii. Measurements of temperature and vapor pressure have been made at various locations, and elevations in the study area, at times coincident with Landsat passes throughout the snow season. Data from the Bishop WSO has been combined with these measurements for utilization of the above mentioned algorithm.

d. Development of topographic longwave radiation algorithms.

i. A method for calculating incoming longwave radiation under clear skies from near surface temperature and vapor pressure has been developed.

ii. Field measurements of incoming longwave radiation have been taken using an Eppley pyrgeometer for verification and calibration of algorithms.

e. Wind interpolations - We have not modeled wind over 3-dimensional terrain. But we have begun to devise some novel methods of indirectly measuring wind, using thermal imagery.

3. Coupling of snowmelt model to a flow model.

a. We have examined the literature on frost penetration and its effect on infiltration rates. During October we plan to install thermistor arrays at several locations in the study area, so that we can monitor soil and snow temperatures during the winter.

b. We have begun to develop a geocoded hydrologic information system for the study area.

c. We have examined literature on flow through snow, and have begun to formulate methods of routing meltwater to the streams.

4. Review of water balance and hydrologic literature to determine potential contributions of remote sensing.

a. We have assembled a set of about 500 pertinent, recent references, and have developed a computerized literature retrieval system around them.

b. Future references can be easily included in our system, and it will shortly be expanded greatly with our collection of soil moisture literature.

c. During the remainder of the first year of the grant period we will expand our review to include other potential applications of remote sensing to hydrologic modeling.

## II. DISCUSSION OF TASKS UNDERWAY

### A. AN ENERGY BALANCE SNOWMELT MODEL FOR RUGGED TERRAIN

One of the major objectives of the project is the extension of an energy balance snowmelt model over rugged terrain. In the initial season we have primarily concentrated on radiation inputs into the snowmelt model, and we have made progress in deriving methods of calculating solar radiation and longwave radiation, and in determining wavelength-dependent reflectance from Landsat data. We have also made a very large number of field measurements of solar and longwave radiation, temperature, humidity, wind speed, and snow temperature and densities; these measurements will be used to calibrate and/or verify our computations. By the end of the first year of the grant we hope to have the radiation algorithms solved. These studies are discussed in detail below.

We have also worked on ways to derive wind velocities over a large area, and ways to couple a snowmelt model to a flow model. In future field seasons we hope to work on these problems.

#### 1. Development and Testing of Wavelength-Dependent Topographic Solar Radiation Algorithms

Many slope radiation models have been developed, but typically they either do not include horizon information, do not calculate reflection from adjacent slopes, or do not subdivide incoming radiation into wavelength bands. In a mountainous, snow-covered area, all of these refinements are essential.

Here we have developed a program which uses the NCIC Digital Terrain Tapes to calculate slope, exposure, and horizon information for every point on a grid (Dozier and Outcalt, in preparation).

To calculate the solar radiation distribution on such a surface, it is necessary to first calculate the beam and diffuse radiation at the range of altitudes in the region. Generally the approach to this problem has been to model the incoming radiation using estimates of the atmospheric aerosol distribution, but these methods are computationally expensive, and aerosol distributions are typically not known.

Our approach is to calculate the wavelength-dependent absorption ( $k_\lambda$ ) and scattering ( $\sigma_\lambda$ ) coefficients and the portion of the radiation scattered forward ( $e_\lambda$ ) from a set of three global radiation measurements with an Exotech Landsat Ground-Truth Radiometer. The method used is to take three measurements, which differ either in orientation or in optical air mass (which varies with solar zenith angle  $Z$ ).

The beam radiation on a surface normal to sun is:

$$S_{\lambda 1} = S_{\lambda 0} \exp [-(k_{\lambda} m_a + \sigma_{\lambda} m_s)]$$

where  $S_{\lambda 0}$  = solar constant in band  $\lambda$   
 $m_a$  = relative absorbing air mass, either ozone or water vapor, depending on  $\lambda$   
 $m_s$  = relative scattering air mass.

The beam radiation on a horizontal surface is:

$$S_{\lambda h} = S_{\lambda 1} \cos Z$$

Global radiation on an unobstructed horizontal surface is (Kondratyev, 1969, p.453):

$$G_{\lambda h} = \frac{(2 - m_s) [S_{\lambda 0} \exp(-k_{\lambda} m_a) \cos Z]}{2(1 - A_{\lambda D}) - (m_s - 2A_{\lambda D}) \exp[\epsilon_{\lambda} \sigma_{\lambda} (m_s - 2)]}$$

where  $A_{\lambda D}$  is the diffuse reflectance in wavelength band  $\lambda$ .

The diffuse radiation  $D_{\lambda h}$  on a horizontal surface is thus:

$$D_{\lambda h} = G_{\lambda h} - S_{\lambda h}$$

The global radiation at a point on a slope, which is the value measured in the field, is the sum of the beam, diffuse, and reflected components:

$$G_{\lambda s1} = S_{\lambda s1} + D_{\lambda s1} + R_{\lambda s1}$$

where

$$S_{\lambda s1} = S_{\lambda 1} \cos Z'$$

$$D_{\lambda s1} = D_{\lambda h} v_f$$

$$R_{\lambda s1} = D_{\lambda h} (1 - v_f) A_{\lambda D} + S_{\lambda 1} (1 - v_f) A_{\lambda DB} + S_{\lambda 1} A_{\lambda B} \sin \theta''$$

where  $Z'$  = solar zenith angle with respect to slope

$v_f$  = view factor, portion of sky seen,  
 $= \cos^2 \{0.5 * [S + (90 - H)]\}$

$A_{\lambda DB}$  = portion of beam radiation which is diffusely reflected

$A_{\lambda B}$  = portion of beam radiation which is specularly reflected

$H$  = mean horizon angle from zenith

$\sin \theta'' = \cos S' \cos Z'' - \cos Z'' \sin Z'' \cos (\phi - \phi')$

$S'$  = slope with respect to opposing slope

$Z''$  = solar zenith angle on opposing slope

$\phi$  = azimuth of sun

$\phi'$  = azimuth of slope

The formulation for  $\sin \theta''$  is from Paltridge and Platt (1976, p.128).



Three measurements of the global radiation, taken either at one time with different orientations, or taken at different times and hence different  $Z$ , lead to three non-linear equations with three unknowns. These are solved using Brown's (1969) method. We will use our extensive radiation measurements to evaluate the effectiveness of this algorithm.

## 2. Shortwave Albedo of an Extensive Snow Cover Derived from Landsat Data

Data inputs to the model consist of the following:

a. Field shortwave radiation measurements: We use Exotech model 100-A "Landsat Ground-Truth" radiometers, with switchable spectral bandpasses identical to MSS bands 4 through 7. The current data base contains measurements taken at intervals of approximately two weeks from 12 February to 31 May 1977, coinciding with Landsat overpasses of the study area. The measurement sequence is described in the previous section. In addition we make a reading of the sky radiation with a  $15^\circ$  field-of-view lens.

b. Landsat computer compatible tapes (CCT's): scenes coinciding with field measurements are a minimum requirement. Ideal coverage requires 3 scenes for each overpass interval of 2 days. Images acquired in the high-gain mode are essentially useless owing to detector saturation over snow.

c. Digital Terrain Tapes: topography of the study area (digitized at 63.5-meter intervals) is obtained on tape from the National Cartographic Information Center.

d. Topographic maps: at 1:62,500 (15') scale, they provide complete coverage of the study area, from which geodetic coordinates of any locatable feature or measurement site may be manually extracted.

e. Ephemeral data: a computer program simulates a specific ephemeris for use in sun angle calculations.

Certain primary transformations must be performed upon each data input. These are:

a. Field shortwave radiation measurements are converted from analog voltage readings to irradiances ( $W m^{-2}$ ) and spectral irradiances ( $W m^{-2} nm^{-1}$ ), by program RADPRNT. This same program organizes the measurements into an indexed file from which they may be accessed according to several sorting parameters. Albedos (beam and global) are calculated by ratioing incoming and outgoing values in subsequent programs.

b. Landsat digital voltage readings (from CCT's) are converted to space upward radiance values ( $R(\text{space})$ ) ( $W m^{-2} sr^{-1}$ ) by the following algorithm.

$$R(\text{space}) = [Vc * (R(\text{max}) - R(\text{min})) / (Ks * Ko)] + R(\text{min})$$

Vc is the calibrated digital voltage for each pixel for each of 4 bands. R(max) and R(min) are band-dependent saturation and threshold radiance values. Ks is a sun-correction constant. Ko is 127 for compressed data from bands 4 through 6, 63 otherwise. In practice this algorithm is implemented as a table lookup by program RADVAL. Saturated values are set to 0, and all zero values are subsequently ignored. RADVAL also reverses the row-order of the image so that the origin is in the southwest corner, conforming to the project standard. Pixel coordinates (sample and line) of selected features are manually extracted from transparencies of the Landsat scene, and verified from computer shade prints produced by program COMPOS. These surface features are evaluated for possible use as ground control points (GCP's) in subsequent image rectification.

c. Digital Terrain Tapes are processed by program DTTORG, which i) resamples the topographic grid to a standard interval (a 100 m interval has been selected as an optimal compromise between resolution and data storage requirements); ii) transposes the grid to a west-to-east major order, beginning at the south-west corner. This resampled and reordered terrain data serves as the base grid to which all other spatial data is registered. In addition, mean slope and aspect are computed and stored for each grid cell.

d. Topographic maps are used to precisely locate field measurement sites and those image grid control points for which reliable image coordinates have been found.

Once primary data transformations are completed, the following secondary transformations are required to complete the database.

a. Relevant portions of the Landsat imagery are rectified to a UTM projection and are resampled to the standard grid interval of 100 m. This is accomplished by various programs in the DIRS package, originally written at NASA/Goddard SFC. The rectification uses original ground control data or is accomplished by registering new imagery to a previously rectified image of the same area.

b. The Digital Terrain data is combined with ephemeral data to generate solar zenith angles for each point on the grid. These are computed relative to absolute and slope zeniths, for the date and time of each image. The slope-zenith angle is combined with ephemeris data and the solar constant to yield a spectral value for incoming shortwave radiation ignoring the atmosphere.

c. Field shortwave measurements and the corresponding computed maxima are input to an atmospheric model described elsewhere in this paper, from which empirical spectral coefficients of absorption, scattering, and fractional forward scattering are in turn used to adjust the computed incoming shortwave radiation throughout the grid.

d. The same atmospheric attenuation factors are now applied to the rectified Landsat radiance values, this time as compensation for the attenuation of upwelling radiance. We now have a grid consisting of corrected upwelling radiance and corrected surface irradiance, computed for each grid cell.

e. The albedo calculated above assumes the surface to be an isotropic (Lambertian) reflector. In fact, snow is an anisotropic reflector with a specular component of reflection that becomes quite pronounced at small angles of incidence (large slope-normal zenith angles). The slope and aspect data contained in the grid, combined with ephemeral calculations, make it possible to introduce a correction to the computed albedo of each cell, based on sun angle, mean slope and aspect of the cell, and look-angle of the MSS. The precise nature of this function has not yet been determined; its dependence upon the age of the snowpack may require an empirically-determined relationship. Also required is a precise determination of which grid cells actually represent unobstructed snow cover, for which an angularly dependent albedo correction would indeed be appropriate.

Of the steps outlined above, the following have been accomplished:

- i. collection of sufficient raw data to begin a meaningful analysis,
- ii. conversion and indexing of field shortwave measurements,
- iii. resampling and regriding of digital terrain data,
- iv. extraction of geodetic coordinates of image control points and field measurement sites,
- v. calculation of ephemeral data (solar zenith angle, solar constant) for entire grid at measurement and/or imaging intervals,
- vi. rectification and resampling of a Landsat subimage,
- vii. calculation of slope, aspect, and horizon profiles for each grid cell.

Of the remaining steps in the model, the following are currently under development (i.e., projected completion within one month):

- i. calculation of "clear-sky" shortwave irradiance over the grid,
- ii. refinement of the atmospheric model and generation of attenuation coefficients,

iii. registration of the rectified Landsat data to the base (terrain) grid.

The major steps in the model remaining to be implemented are:

i. calibration of the Landsat and surface radiance values with the atmospheric factors, and subsequent albedo calculation,

ii. development of a workable angular correction for snow albedo.

### 3. Development and Testing of Longwave Radiation Algorithms

The model under development is structured as follows:

a. A digitized grid of elevations is formed for the study area from Digital Terrain Tapes (DTT'S) using the program DTTORG. The grid resolution is variable and the optimum resolution is determined for each model application. Mean horizon angles and thermal view factors are calculated from terrain data for each grid point by routine HORTAB (Dozier and Outcalt, in preparation):

$$Vf = \cos^2[(90-H)/2]$$

where: Vf = thermal view factor  
H = mean horizon angle from grid point

b. Field data and data from Bishop WSO are combined by routine LNGDAT. Measurements of air temperature, wet bulb temperature, air pressure, and elevation are combined sequentially with field measurements from a particular model run period. These are used as a reference for calculating air pressure over the study area and for the establishment of temperature and vapor pressure lapse rates. Pressure is calculated for each grid point using Bishop station pressure and a standard temperature lapse rate ( $-7^{\circ}\text{K km}^{-1}$  is typical of the study area). Note that this equation is reasonably insensitive to minor variations in the temperature lapse rate due to the extreme variation of pressure with elevation (Kantor and Cole, 1965):

$$P_a = P_o * \exp[(-g*m)/(R*\Gamma) * \ln\{(T_o + \Gamma*(z-z_o))/T_o\}]$$

where: Pa = pressure at elevation z  
Po = pressure at Bishop  
g = acceleration of gravity  
m = molecular weight of dry air  
R = molecular constant for an ideal gas  
Γ = temperature lapse rate  
z = elevation of grid point  
zo = elevation at Bishop WSO  
To = temperature at Bishop WSO

c. Temperature and vapor pressure lapse rates are established for the model run period over the study area from field measurement data. Wet bulb depression ( $T_a - T_w$ ) is converted to vapor pressure from station pressure and the psychrometric equation (Byers, 1974):

$$e(a) = e(s) - [(C_p * P_a) / (.622 * L)] * (T_a - T_w)$$

where:  $e(a)$  = vapor pressure  
 $e(s)$  = saturation vapor pressure  
 $C_p$  = specific heat of dry air at constant pressure  
 $L$  = latent heat of vaporization  
 $T_a$  = air temperature at  $z$

Temperature is converted to potential temperature to simplify computations (Cramer, 1972):

$$\theta = T_a * (1000/P_a)^{**}[R/(m * C_p)]$$

Field measurements of temperature and vapor pressure, which are irregular both spatially and temporally, are expanded to a regular grid by program NEWGRD using the following procedures:

i. Gravity model forms an irregular grid from X/Y relationship of elevation and time.

ii. Laplacian transform smooths the irregular grid (Note: procedures a) and b) were developed by S. Outcalt)

iii. A bicubic spline interpolation resamples the irregular grid at specified time and elevation intervals forming a regular grid (de Boor, 1962; Rogers et al, 1976).

These grids of  $[(\partial\theta/\partial t)$  by  $(\partial\theta/\partial z)]$  and  $[(\partial e(a)/\partial t)$  by  $(\partial e(a)/\partial z)]$  are used to determine  $\theta$  and  $e(a)$  for each point in the elevation grid. Potential temperature is converted back to air temperature for each grid point by:

$$T_a = e / (1000/P_a)^{**}[R/(m * C_p)]$$

d. Program INFLUX calculates the following:

i. Effective clear sky emissivity for every grid point using Brutsaert's (1975) technique corrected for diminished pressure and optical path length:

$$\epsilon(a) = 1.24[e(a)/T_a]^{1/7}$$

ii. Incoming longwave radiation for every grid point using output from the above equations:

$$I(i) = [\epsilon(a) * Ta^4] * [1-Vf] + [\sigma * Ts^4] * Vf$$

where:  $\sigma$  = Stefan-Boltzmann constant  
Ts = surface temperature

Surface temperature is approximated from an interpolated mean of field measurements.

e. The grid of incoming longwave radiation flux is:

i. Written to disk for input to energy balance snowmelt model.

ii. Plotted as a contour map over the study area.

iii. Plotted as a three dimensional surface over the study area.

The model will be calibrated and tested for accuracy by the following procedures:

a. Bishop WSO data will be used to calculate pressure over the study area and to initialize the model for Ta, e(a), and Pa.

b. Field measurements of Ta and e(a) will be used to determine accurate temperature and vapor pressure lapse rates for determining effective atmospheric emissivity.

c. Pyrgometer measurements of incoming longwave radiation will be used:

i. To run a sensitivity analysis of input parameters Ta, e(a), their lapse rates, and Pa, the grid resolution, and the time interval, to improve the model efficiency and the cost-effectiveness of field data collection.

ii. To make a first order determination of the effect of cloud and forest radiation on incoming longwave radiation.

iii. To evaluate model accuracy statistically.

#### 4. Possible Approaches to Wind Interpolation

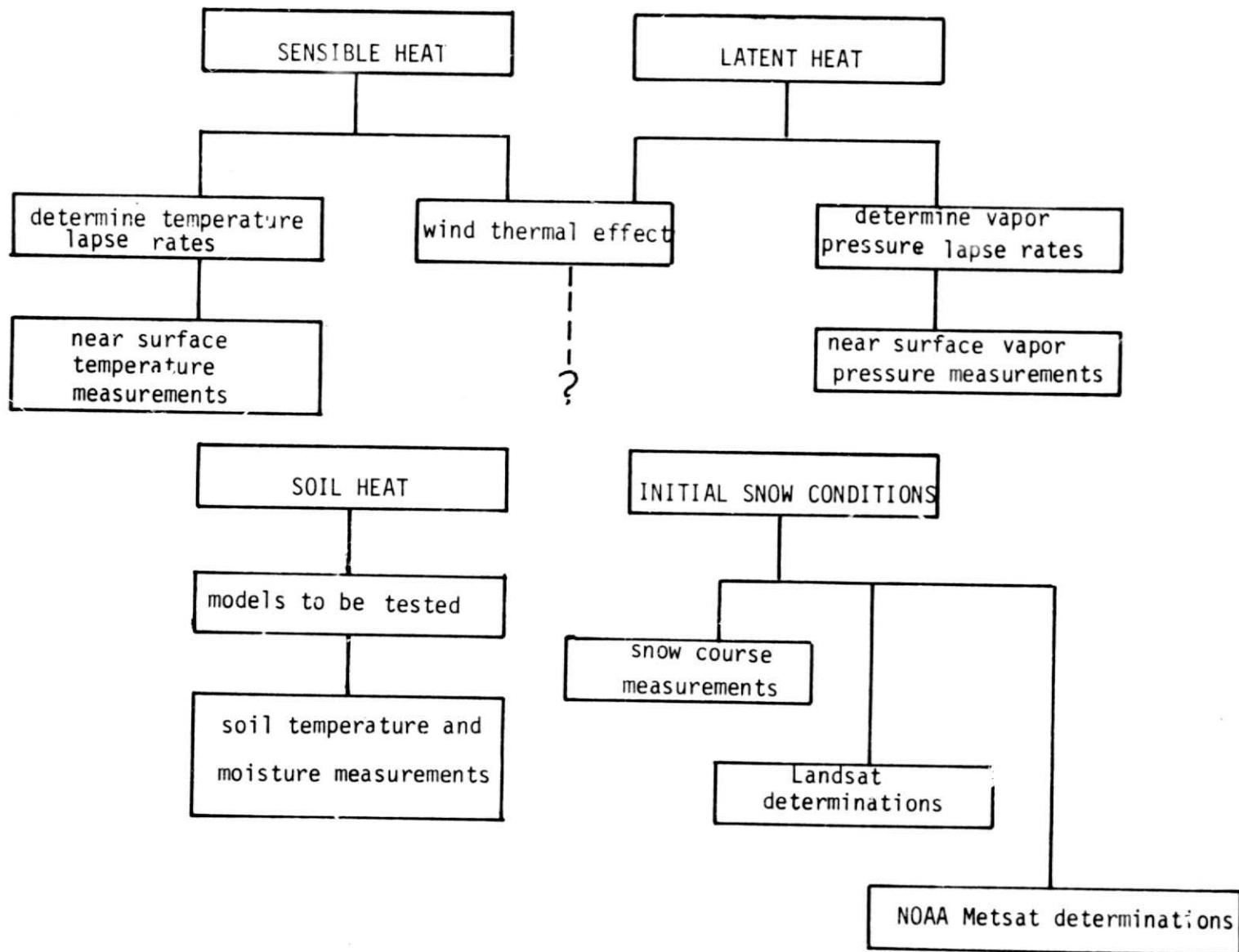
One of the knotty problems which continues to face us is the interpolation of wind over complicated three-dimensional terrain. While flow over simplified, two-dimensional topography has been simulated, as has flow at higher elevations in the atmosphere, calculation of surface turbulent exchange remains a serious problem. During the

next seasons, we intend to try to utilize thermal data from Landsat-C, HCMM, and Tiros N to investigate the wind field. Our approach will be to invert the snow surface temperature model. Specifically, during non-melting conditions, if wind speed, roughness length, radiation etc. are known, a snow temperature profile is one of the outputs of Anderson's (1976) model. The existence of thermal satellite data would allow us to measure surface temperature, and solve for the turbulent transfer coefficient, which is related to wind speed.

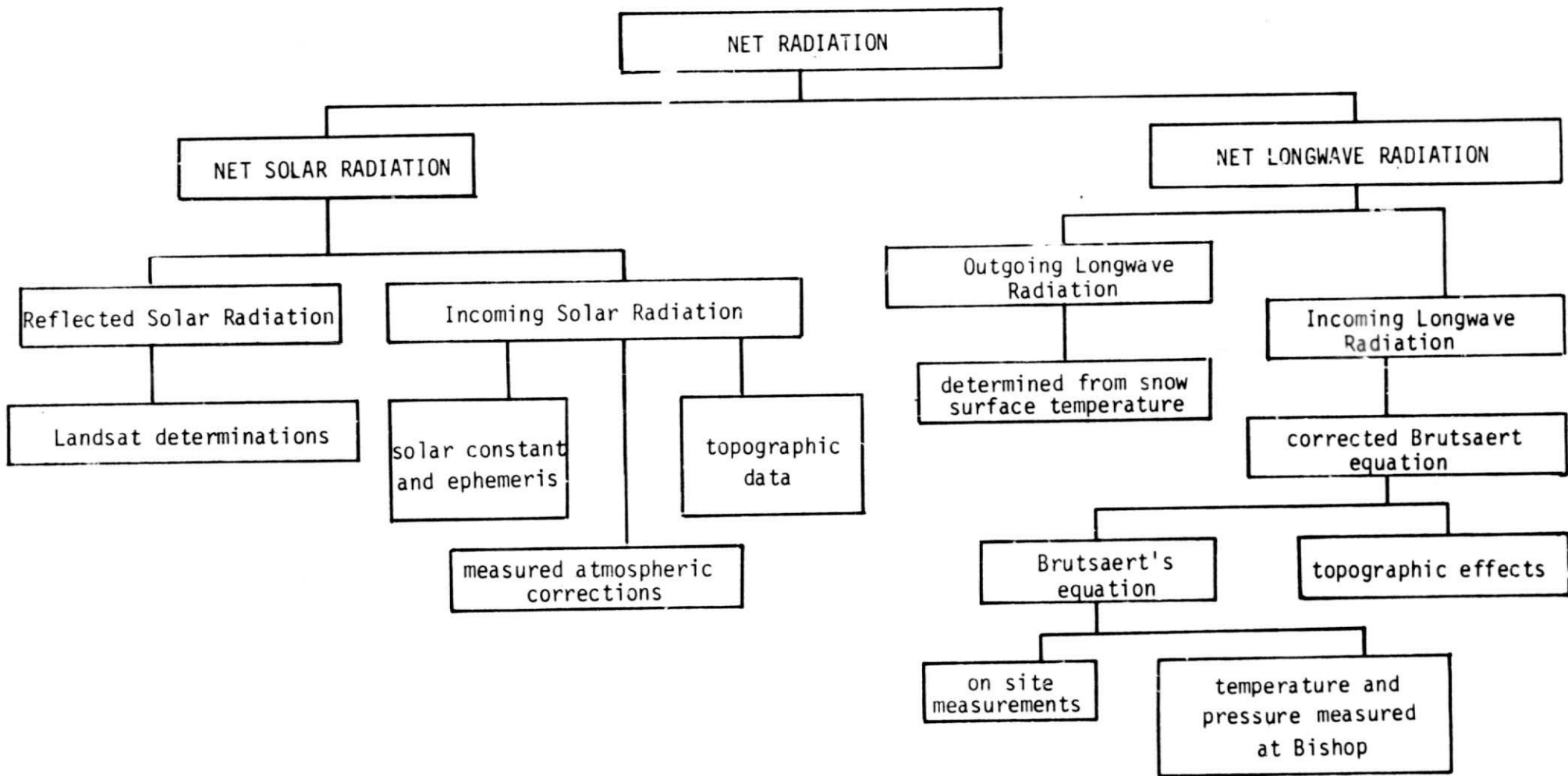
In order to properly carry out this experiment, we would need thermal data 24 hours apart for the same area. For Landsat-C or HCMM data we could use the sidelap zone, or we could use Tiros N data directly. Landsat-C would provide the best resolution, but the temperature response of the instrument is not as precise. HCMM data may not be readily available. In any case we would carry out simultaneous ground measurements, to filter out atmospheric effects.

Once several spatial measurements under different meteorological conditions were obtained, we could estimate area-wide wind distributions for these conditions.

SNOWMELT MODEL INPUTS TO ENERGY BALANCE EQUATION







## B. COUPLING SNOWMELT MODEL TO A FLOW MODEL

### 1. Review of Literature on Frost Penetration and its Hydrologic Effects

We have reviewed the general properties and processes of seasonally frozen ground emphasizing relatively coarse soils, since preliminary research of the mountainous portion of the test area indicates the predominance of rocky sandy soils (Anderson, 1946, Storie, 1957). Heat and moisture exchange between the snowpack and ground can influence the timing of snowmelt. Conditions on the surface and in the ground can also influence the timing and rates of runoff.

The presence of bonded concrete frost represents an impermeable layer at the depth of ice formation (Dingman, 1975). Although concrete frost is probably rare in the Sierra, it may occur in years when initial snowfall is late. Other types of frost may increase infiltration capacity or leave it unaltered (Trimble, et al., 1958, Schumm and Lusby, 1963). Outcalt (1971, 1976) has developed computer simulation of the formation of frost with varying morphology, and Harlan (1971, 1973) presents a coupled heat-fluid transport model which describes the process of infiltration into a freezing or frozen soil with given surface boundary conditions. The process of infiltration is also numerically described in static phases by a numerical model developed by Alexeev et al. (1972) who also present a simplified dynamic model shown to give good results in sandy soils. The models by Harlan (1971, 1973) and Alexeev et al. (1972), relatively recent and theoretically based, lack extensive empirical validation. These models, particularly that of Harlan (1973) may be suitable for insertion as subroutines in an overall surface energy budget simulator (e.g. Outcalt and Carlson, 1975).

In order to test the ability of these various models to calculate soil temperatures and frost penetration, we plan to install arrays of thermistors and soil moisture blocks at a few locations within the study area this fall. These will enable us to rapidly measure temperature and moisture gradients within the soil (and snow) when we visit the sites.

### 2. Development of Geocoded Hydrologic Information System

We have begun to assemble a geocoded hydrologic information system for the study area. The drainage basins have been classified into a hierarchy based upon drainage area, and we are digitizing the boundaries. Once the boundaries are digitized, we will be able to create a file for a given basin which contains a variety of data for every point in the basin. Static data would include topographic information such as slope, exposure, horizons, elevation, and vegetative cover. Temporal data would include solar

radiation for a given data, Landsat radiance, reflectance, and whether snow-covered or not.

We have not yet agreed on the proper format for this information system, and plan to delay doing so until after a NASA-funded conference on geobase information system formats, to be held in Santa Barbara this month, is concluded.

### 3. Development of Flow Model for Snowmelt

In the Southern Sierra Nevada almost all of the runoff is from snowmelt. Under extreme conditions, such as occurred during this last winter, snowmelt models based on regression analysis fail to adequately predict snowmelt runoff. Energy balance snowmelt models can predict runoff accurately under extreme (drought or flood) conditions, but to be used operationally to improve development or regulation of water resources, they must be coupled to existing or modified streamflow models.

Thus the energy balance snowmelt model must be coupled to a streamflow model. Once snow has begun to melt the following must be evaluated: 1) infiltration and runoff beneath the snowpack; 2) moisture flow in saturated soil below the snow line; 3) soil vapor losses. In addition problems of differences in the resolution between the snowmelt model and the flow model must be overcome. We see our primary problem in the estimation of flow from the snow to the nearest stream. Once in the stream, existing flood routing algorithms are probably sufficient, at least for an initial approximation to the runoff distribution. In the coming field season we plan to use our arrays of thermistors and soil moisture blocks, plus thermal imagery from Landsat-C, HCMN (if available), and NOAA environmental satellites to estimate water characteristics of the snowpack.

## C. LITERATURE REVIEW ON REMOTE SENSING APPLICATIONS TO HYDROLOGIC MODELING

### 1. Development of Bibliography and Computerized Retrieval System

Thus far our efforts on this task have been devoted to gathering articles on the specific problems that we have confronted, and to developing a computerized information retrieval system for this bibliography. In comparison to other literature data bases, this one is quite small and rather specialized. At present it deals only with those aspects of hydrologic modeling where we have investigated the role of remote sensing.

The purpose of the literature retrieval system is primarily to organize the information in the library. The first task was to define a list of keyword topics into which the articles and books could be categorized. For each article, book, and proposal a card was made listing the author or authors, the title, the date of publication, the publication title for a journal or the publisher for a book, the topic or topics of the entry, and any other relevant information. The cards are filed alphabetically by author and kept as a complete catalogue of the library. They are computerized in order to facilitate their rapid sorting by author, topic, or publication.

CARDCAT, the card catalogue program, is capable of maintaining a library of up to about 30,000 bibliographic entries. (At present only about 500 entries are supported.) It can add entries to this library and link them together in four different ways. Thus the user can obtain a listing of the entire data base alphabetically by author, of a given topic alphabetically by author, of a given author chronologically (latest first), or of a selected entry by specifying a title. Entries may be deleted at any time. The user may also specify unions and intersections of topic listings so that subtopics may be used in the cataloguing process. For example, entries under subtopic "a" may be obtained. A listing of all entries under both topics "B" and "a" would contain those entries under topic "B," subtopic "a." By requesting a listing of all entries in the union of topics "A" and "B" the user would obtain the entire list of entries for both topics. Finally, the user may obtain a listing of all entries by a single author. When not executing, the CARDCAT program stores the data file on disk.

### 2. Future Remote Sensing Applications to Hydrologic Modeling

Current inputs to hydrologic modeling from remote sensing have mostly been limited to presence or absence of hydrologic phenomena. This is evident in the extensive use of remote sensing data for mapping snowcover areal extent

(e.g. Barnes and Bowley, 1970; Siefert et al, 1975; Rango, 1975). Improved accuracies of runoff prediction from the use of this application have been striking (Rango and Salomonson, 1975).

However, most operational hydrologic models are lumped parameter models, usually based on one or more convenient indexes (such as snow course measurements). Remote sensing data offers high resolution, multispectral information that cannot be effectively used by such models. With the development of distributed parameter hydrologic models, such as an energy balance snowmelt model, comes the opportunity to more fully utilize remotely sensed data.

Techniques developed for remotely sensing thermal characteristics of the surface and the atmosphere have been restricted to oceanic regions due to noise problems from terrain and the differential thermal properties of land materials (Yates and Bandeen, 1975). It is hoped that these techniques can be extended over an alpine snowfield where the thermal properties of the surface are known and where the terrain effects can be filtered. As new remote sensing devices become operational, such as the HCMM and Landsat-C, the effective use of thermal data inputs for hydrologic modeling will become more important (Lockheed Electronics Co., 1977). In this regard, we will be reviewing literature on the following topics:

- i. Remote determination of soil and snow moisture content.
- ii. Plant canopy temperature determination and measurement.
- iii. Determination of cloud cover thickness, temperature, and water content.
- iv. Techniques for thermal mapping of snowfields; especially mapping the isothermal ( $0^{\circ}\text{C}$ ) portions of a snowfield.
- v. Determination of atmospheric temperature and vapor pressure profiles.

### III. SOFTWARE DEVELOPMENT - NASA HYDROLOGY PROJECT PROGRAM STRUCTURE

The NASA hydrology project programs are designed to perform specific tasks, and to write the output in a file which may in turn be accessed by other programs. In order that the hassles involved be minimal, they must be standardized in output format.

By agreement then, we adopt the following standards:

1. With some exceptions, output files are in binary, and are written as sequential files on tape or disk.
2. The first record should contain the dimensions of the output file (e.g. NX by NY for a grid) and other appropriate information, such as latitude and longitude, grid spacing, etc.
3. Gridded information is written by row, starting from the SW corner. Extensive existing software (e.g. DIRS) which does not use this convention should not be rewritten though. Instead, the output files can be subsequently re-formatted.

All programs should be briefly documented. The documentation should contain the input specifications, a description of the methods used, and an explicit description of the output records. Programs should also give a sample print-out of the output data set. Because we use a variety of languages, we must take care to make data sets compatible. Load modules for complete programs should be stored in the RDS HYDROLOGY.PROJECT.PROGLIB on D10300 unless you have a particular reason for putting them elsewhere. This disk should be otherwise used for data sets only.

#### I. Topographic analysis.

A. DTTORG - selects data from digital terrain tapes and writes into a disk or tape file. Options for interpolation and smoothing.

B. TERRAIN - calculates slope, exposure, horizons, latitudes, longitudes and elevations. Writes into file. Can be subgrid of that written by DTTORG.

#### II. Solar radiation.

A. RADPRNT - prints out in table format measurements with Landsat radiometer. Writes results into sequential indexed file for input to other solar radiation programs.

E. SOLGRD (not yet complete) - calculates solar radiation. Numerous options:

1. Selected points in selected wavelengths at selected time step. Print out. Used for verification and calibration.
2. Selected wavelength intervals at specified time over entire grid. Used for comparison with imagery.
3. Selected wavelength intervals at specified time step over entire grid. Used for model input.
4. Selected integrations over desired intervals.

Options 3 and 4 may be in terms of net solar radiation as well as incoming. Program uses either estimated or measured reflectances; estimated or measured absorption and scattering coefficients and portion of radiation scattered forward. Interruption by canopy cover can be specified for all options.

### III. Longwave radiation.

A. LONGPRNT - prints out in table format longwave radiation measurements.

B. SPACSAVR - (formats measurements for input to other programs); writes binary data to disk in packed format.

C. TZTEMP - time/elevation interpolation to estimate humidity and temperature at all elevations and times.

1. Calculates lapse rates for temperature and humidity.
2. Adds pressure, temperature, and humidity measurements from Bishop weather station.
3. Plots time-space graphs for temperature and humidity.
4. Writes interpolated temperature and humidity to disk for TZGRID.

D. INFLUX - calculates longwave radiation from temperature, humidity, and topographic data. Uses measurements for calibrations. Options:

1. Selected points at selected time step used for verification and calibration.

2. At specified time over entire grid.
3. At specified time step over entire grid. Used for model input.
4. Selected integrations over desired time intervals over entire grid. Used for model input.

IV. Temperature and humidity data.

A. TZGRID - coarse model. Uses TZTEMP to specify temperature and humidity values at every grid point for every time step.

V. Wind information - not yet developed.

VI. Snowmelt modeling.

A. SNOWBAL - (from Anderson, 1976) uses input from previous programs to run snowmelt model for all grid points.

VII. Satellite data analysis programs.

A. DIRS - NASA program for rectification, rotation, and printer display of Landsat data. System elements:

1. COMCCT - Converts rectified image or subimage from composite to CCT format.
2. COMPOS - Reformats CCTs into composite tape format; produces shade prints; does edge image correlation.
3. DICOSYS (not yet implemented) - Accepts film recorder format image tapes and applies annotation contrast and expansion operations to the image; produces film recorder output tapes.
4. MAPX (not yet implemented) - Extracts single band quadrilateral subimage areas from composite format rectified image tape.
5. MAP2X - Rectifies quadrilateral subimage areas from composite tape with GEOM file and writes output in composite or film recorder format.
6. QUIKLOOK (not yet implemented) - Accepts composite format image tapes and produces film recorder format output image tapes with optional geometric, radiometric, and annotation enhancements.



7. RECTFI - Cross checks control points (GCPs and CCPs); computes global mapping functions; creates interpolation grid; writes GEOM file on composite tape; optionally rectifies full image.

8. REFRAME - Vertically mosaics unrectified Landsat scenes which are contiguous.

9. REGISTER (not yet implemented) - Converts correlation control points into pseudo GCPs by computing UTM coordinates at point and storing point in GCP format.

10. SIATDUMP (not yet implemented) - Extracts image format center time and attitude estimate from SIAT file.

B. RADVAL - reformats DIRS output and converts to radiance values.

VIII. Mapping programs, for interpolation and display of results.

A. DTTMAP - maps output from DTFORG, as contour maps or perspective plots.

B. NCAR graphics package (not yet implemented) - powerful set of subroutines for graphic output on Calcomp plotter.

C. NEWGRD - transforms irregularly spaced data into square or rectangular grid by using gravity model to form irregular grid and smoothing with Laplacian; bicubic spline interpolation then creates grid.

IX. Miscellaneous subroutines, in addition to those in the IMSL package. These are imbedded in the above programs, but others may find them useful separately.

ANGIN - solar geometry for slope

ASPECT - slope and exposure for point on grid

COEFIG - calculates absorption and scattering coefficients and portion of radiation scattered forward from set of three global radiation measurements

COOLER - Fast Fourier Transform

CSTEP - Fourier Transform of a step function

EPHEM - declination, radius vector, and equation of time as function of date

HORTAE - calculates horizon angle file for point in grid

IDMSS - converts degrees, minutes, seconds (as single integer) to seconds

MOVE - Moves one vector into another (in Assembler - very fast)

NEWTON - root finding by Newton's method

RSINTG - Rayleigh scattering coefficient averaged over specified wavelength range

RSINTE - Rayleigh scattering coefficient at specified wavelengths

SATW and SATI - saturation vapor pressure over water and ice

SCINTG - integrated solar constant in specified wavelength range

SCINTE - solar constant at specified wavelengths

SKYFAC - diffuse solar radiation and atmospheric thermal radiation view factor

SNPATH - sun position for date, latitude, and time

ZERO - zeroes a vector (in Assembler - very fast)

ZPRESS - calculates pressure as a function of elevation, temperature, and lapse rate

IV. ACCOMPLISHMENTS FORESEEN BY END OF FIRST YEAR OF GRANT  
AND RECOMMENDATIONS FOR FURTHER WORK

Prior to the end of the first year of the grant, we foresee completion of the following tasks:

1. The clear-sky solar radiation model should be developed, with the inclusion of reflectance from adjacent slopes. The model will be adequately tested.
2. A method of determining snow albedo from Landsat data will be completed and tested.
3. A method of calculating clear-sky longwave radiation at varying altitudes will be completed and tested.
4. A geocoded hydrologic information system will be developed for the study area.

Further tasks which we hope to accomplish in the next two field seasons are:

1. Interpolation of Soviet satellite imagery of the Fergana Valley test site.
2. Review of hydrologic modeling literature, to evaluate what model changes are needed for remote sensing to play a more meaningful role.
3. Development and testing of frost penetration calculations for the study area.
4. Development of algorithms to couple snowmelt model to flow model.
5. Use of thermal imagery from Landsat-C, HCMM, and NOAA environmental satellites such as TIROS N to better estimate longwave radiation from clouds and forests.
6. Use of thermal imagery to estimate wind distribution over rugged terrain.

V. REFERENCES

- Alexeev, G.A., I.L. Kaljuzhny, V.Ya. Kulik, K.K. Palova and V.V. Romanov, 1972, Infiltration of snowmelt into frozen soil. Paper presented at Intl. Symposium on the Role of Snow and Ice in Hydrology, Banff, Alta., Canada, Sept. 1972.
- Anderson, H.W., 1946, The effect of freezing on soil moisture and on evaporation from bare soil. EOS: Trans. of Amer. Geophys. Union, 27, 863-870.
- Barnes, J.C., and Bowley, C.J., 1970. Use of ERTS data for mapping snow cover in the western United States. Paper presented at National Fall Meeting of AGU, San Francisco, CA, Dec. 1970, 885-862.
- Brown, K.M., 1969. A quadratically convergent Newton-like method based upon Gaussian elimination. SIAM Jour. Numerical Anal. 6, 560-569.
- Brutsaert, W., 1975. On a derivable formula for longwave radiation from clear skies. Water Resources Research, 11, 742-744.
- Byers, H.R., 1974. General Meteorology. New York, McGraw-Hill, 461 pp.
- Cramer, O.P., 1972. Potential temperature analysis for mountainous terrain. Jour. Appl. Met. 11, 44-50.
- de Boor, C., 1962. Bicubic spline interpolation. Journal of Mathematics and Physics 41, 212-18.
- Dingman, S.L., 1975, Hydrologic effects of frozen ground, U.S. Army CRREL, spec. rpt. 218.
- Dozier, J., and Outcalt, S.I., (in preparation). An approach toward surface climate simulation in rugged terrain.
- Harlan, R.L., 1971, Water transport in frozen and partially frozen porous media. In Runoff from Snow and Ice, vol.1, Symposium no.8, Quebec, Can. May 1971; Inland Waters Branch, Dept. of Energy, Mines and Resources, Ottawa Canada.
- Harlan, R.L., 1973, Analysis of coupled heat-fluid transport in partially frozen soil. Water Resources Res. 9(5) 1314-1323.
- Kantor, A.J., and Cole, A.E., 1965. Atmospheric pressure up to 90 km. in Valley, S.L., (ed.), 1965. Handbook of Geophysics and Space Environments. AFCRL.
- Kondratyev, K.Ya., 1969. Radiation in the Atmosphere. Academic Press, New York, 912 pp.

- Lockheed Electronics Co., 1977. The status of environmental satellites and availability of their data products. NASA technical report; Earth Observations Division, NASA/Johnson Space Center.
- Outcalt, S., 1971, An algorithm for needle ice growth. Water Resour. Res., 7, 394.
- Outcalt, S. and J.H. Carlson, 1975, A coupled soil thermal regime surface energy budget simulator. Proceedings: Conference on Soil-Water Problems in Cold Regions, Calgary, Alberta, Canada, 1-33.
- Outcalt, S., 1976, Numerical model of ice lensing in freezing soils. Proceedings: Second Conference on Soil-Water Problems in Cold Regions, Alberta, Canada. 63-75.
- Paltridge, G.W., and Platt, C.M.R., 1976. Radiative Processes in Meteorology and Climatology. Elsevier Scientific Publ. Co., Amsterdam, 318 pp.
- Rango, A., 1975. An overview of the Applications Systems Verification Test on snowcover mapping. Operational Applications of Satellite Snowcover Observations, NASA SP-391; 1-12.
- Rango, A., Salomonson, V.V., and Foster, J.L., 1975. Employment of satellite snowcover observations for improving seasonal runoff estimates. Operational Applications of Satellite Snowcover Observations, NASA SP-391; 157-174.
- Rogers, D.F., and Adams, J.A., 1976. Mathematical Elements for Computer Graphics. McGraw-Hill Book Co.
- Schumm, S.A., and G.C. Lusby, 1963. Seasonal variation in infiltration capacity and runoff on hillslopes in Western Colorado. Journal of Geophysical Research, 68, 3655-3666.
- Seifert, R.D., Carlson, R.F., and Kane, D.L., 1975. Operational applications of NOAA-VHRR imagery in Alaska. Operational Applications of Satellite Snowcover Observations, NASA SP-391; 143-156.
- Storie, F.E., and F. Harradine, 1957. Soils of California. Soil Science, 85, 207-228.
- Trimble, C.R. Jr., R.S. Sartz, and R.S. Pierce, 1958. How type of soil frost affects infiltration. Journal of Soil and Water Conservation; 13, 2, 81-82.
- Yates, H.W., and Bandeen, W.R., 1975. Meteorological applications of remote sensing from satellites. Proc. IEEE 63: 1, 148-163.